

Geospatial approach to elucidate anomalies in the hierarchical organization of drainage network in Kuttiyadi River Basin, Southern India

Thulasi Veedu SWETHA (✉)¹, Girish GOPINATH (✉)^{2,3}, Arun BHADRAN⁴, Arjun P²

¹ Department of Geology and Environmental Science, Christ College, Kerala 680125, India

² Geomatics Division, Centre for Water Resources Development and Management, Kerala 673571, India

³ Department of Climate Variability and Aquatic Ecosystems, Kerala University of Fisheries and Ocean Studies, Kerala 682508, India

⁴ Earthquake Geology Division, Geological Survey of India, NER Shillong 793014, India

© Higher Education Press 2022

Abstract An assessment of anomalies in the hierarchical organization of the drainage network in the Kuttiyadi River Basin (KuRB), Kerala, has been performed by considering various morphometric parameters such as bifurcation index (R), hierarchical anomaly index (Δa), hierarchical anomaly density (ga), and stream gradient index (SL) in a geographical information system (GIS) platform. Further, a digital elevation model (DEM) of the area has been generated from Cartosat stereo pair data at 2.5-m resolution. The computed quantitative information about drainage characteristics reveals the highest drainage anomaly is observed in sub-watersheds (SW) III and IV. It is observed that neo-tectonic activity caused the development of younger stage drainage patterns of structural controls in the sub-watersheds of this river basin. The tectonic activity-induced diffusion, high energy fluvial erosion, and anthropogenic interferences altered the hierarchical organization of the drainage network of the sub-watersheds in mature to old stages of geomorphic evolution. The results of finding validated with asymmetry factor and ratio of the hierarchical index (Δa) with hierarchical anomaly number (A), bifurcation index (R), direct bifurcation ratio (R_{db}), stream gradient index (SL), and denudation index ($\log Tu$). From the denudation index analysis, the sediment yield of the river basin is identified as $0.67 \text{ t}\cdot\text{km}^{-2}\cdot\text{yr}^{-1}$. Moreover, the asymmetric factor (AF) in the KuRB shows the imprints of Paleo–Neo Proterozoic crustal tilting toward a NNW–SSE direction.

Keywords river basin, hierarchical anomaly, bifurcation index, stream gradient index, denudation index, Cartosat-1 DEM

Received February 16, 2021; accepted May 26, 2021

E-mail: tvthulasy@gmail.com (Thulasi Veedu SWETHA)
gkufos@gmail.com (Girish GOPINATH)

1 Introduction

Geomorphology of the earth is made by many nature processes, in which the rivers play vital role by making enormous structures in a simplified view with complex tectonic imprints, which is hidden in a broad canvas known as a drainage basin. Deciphering the geomorphic indices and anomalies of a river basin are the most reliable proxy for the tectonics and their impact in catchment areas (Keller and Pinter, 2002; Kumar and Duarah, 2019, 2020). These proxies can be examined through quantitative and qualitative methods, in which geospatial technology has proven to be an extremely powerful tool for the analysis of various drainage morphometric parameters. The morphometric parameters of both active and passive tectonic areas will give different patterns of geomorphological indices, which are expressed in empirical relations made by various authors such as Marta et al. (2008), Hamdouni et al. (2007) to understand the tectonism of the region. Drainages are the surface amplifications of earth's internal brittle and ductile deformations such as faults, folds, and shears, which make entanglements in drainage patterns in corresponding to lithology (Schumm et al., 2000; Burbank and Anderson, 2001). Systematic studies of drainage will give insight to understand the tilting or upliftment of a river basin/watershed, geological stage of development, and geomorphic process involved in its inception. This information can summit the neotectonic activity and geomorphic anomalies occurring in the area (Ghosh and Sivakumar, 2018). The characteristic pattern and life histories of drainages in youthful stage, mature stage and in old stage and its deviations from their normal life histories, especially in the form of various drainage anomalies have been inferred to be the indications of the effect of tectonic scenario (Ramaswamy et al., 2011). The

quantitative analysis of anomalies in drainage network within a river basin or watershed can decipher processes such as erosion, diffusion, mass movement, neotectonic activities, or anthropogenic interferences (Avena et al., 1967). The hierarchical anomalies of drainage network can provide numerical measures about the interpretation of landscape dissection and runoff, structure and effect of tectonism, and their etching over the surface. Rivers are very sensitive to tectonic activities, sediment diffusion, surface runoff in a drainage basin, etc., and these types of studies are essential to identify the geomorphic effect and its impacts in a river basin and to implement measures for target-oriented micro watershed management (Ambili and Narayana, 2014; Vijith et al., 2017; Bhadrans et al., 2018).

The hydrological pattern of the catchment is mainly controlled by factors such as climate, and the various morphometric characteristic too. The classification system of the stream network initiated by Horton (1941) has utilized to determine the holistic stream properties, such as the analysis of drainage network development and its morphometric analysis. The effect of neotectonic activities in the drainage network development can identify from the lineaments, stream channel orientation rectangular drainage pattern, high bifurcation ratios, and low values of form factor (Ramaswamy et al., 2011). The geographical information system (GIS) application for the investigation and estimation of a river basin morphometry and extraction of relief parameters from the Digital Elevation Model (DEM) data has massive utility for watershed development and management (Praveen et al., 2019). The measurement of DEM was carried out to derive river sinuosity index of 15 watersheds of Meenachil River, Kerala, India and interpreted that changes in sinuosity values are due to influenced tectonic features (Kumar et al., 2014). To extract a slope map for groundwater potential zone identification of the Kuttiyadi river basin, the high resolution Cartosat-1 DEM data used a slope with 0–5%, 5%–15%, 15%–25%, and > 25% obtained for the area (Swetha et al., 2017). Jesiya and Gopinath (2018) used integrated MCDM-GIS techniques to assess the groundwater potential index of urban and peri urban zones of Kozhikode district, Kerala, the slope map of the area generated from DEM data, the coastal alluvium formation is interpreted as very good groundwater potential zone. Bilous et al. (2020) utilized DEM data for landscaping modeling through the spatial structural and morphometric parameters analysis of the terrain. To estimate the erosion status of the Amanikere Basin, Dakshina Pinakini Basin, Karnataka, Cartosat-1 DEM data have been used to identify morphometric and hypsometric parameters and interpreted that basin is in a mature stage of development (Dikpal et al., 2017). Gopinath et al. (2014) extracted watershed boundaries and a drainage network of a tropical river basin from SRTM DEM data and compared it with toposheet data to highlight the wide application and importance of accuracy and quality in raw DEM.

To understand the drainage anomalies and their tectonic kinematics, a tropical river in the southern passive peninsular eastern slope of Western Ghat is selected. Quantitative and descriptive morphometric analysis of the drainage network and the tributary of Kuttiyadi River Basin (KuRB) were studied by Gopinath et al. (2014 and 2016) and the study brought out that the main causative factor of land form evolution in KuRB is the fluvial geomorphic process. In the present work, the high values of drainage parameters (drainage density and drainage texture) and ruggedness number in the sub-watersheds and their anomalies are studied in-depth. Various authors addressed the active/neotectonic fabrics in the adjacent river basins of KuRB (Vijith and Satheesh, 2006; Manu and Anirudhan, 2008; Rekha et al., 2011). To address the drainage network anomalies and the associated activity in the KuRB as a whole, the bifurcation index (R), hierarchical anomaly index (Δa), hierarchical anomaly density (ga), and stream gradient index (SL) are calculated empirically along with asymmetry factor analysis.

2 Regional settings

Geographically, Kuttiyadi River Basin lies between latitudes 11°30'N and 11°44'N and longitudes 75°34'E and 75°58'E that enjoys a tropical humid climate. The highlands of the Kuttiyadi River Basin is a part of the Western Ghats and the Kuttiyadi River is mounting from the Narikota Ranges (at an elevation of 1641 m above MSL) on the western slopes of the Wayanad Hills and drains into the Arabian Sea at Kottakal. This west-flowing river is 74 km long and drains an area of 676 km² (Fig. 1).

The present study area falls within the western part of charnockite dominated Nilgiri Block of Southern Granulite Terrain. KuRB is bounded in the north by Coorg Block and south by Madras Block and these crustal blocks are sutured by two semicircular crustal scale shear zones, Moyar and Bhavani, respectively. These shear zones are collision sutures developed in the Gondwana super continent and reactivated during Pan African period (Santosh et al., 2015) and the rocks in this area are under dextral kinematic regime (Prasannakumar and McCaig, 2016) (Fig. 2(a)). In KuRB, crystalline rocks of charnockite and gneisses; which are dissected by younger rift drift associated Dykes of Mesozoic, coastal area covered by recent sediments and tertiary laterites (Fig. 2(b)). Lineaments in the study area are 1) NW–SE to WNW–ESE, 2) NNW–SSE to N–S, and 3) ENE–WSW (Fig. 1). These lineament directions can provide evidence on deformation which the study area has undergone (Nair, 1990). The earthquake epicenter data studies by Soman (2013). Rajendran et al. (2009) implies that, the lineaments in this area are tectonically active even in the present time.

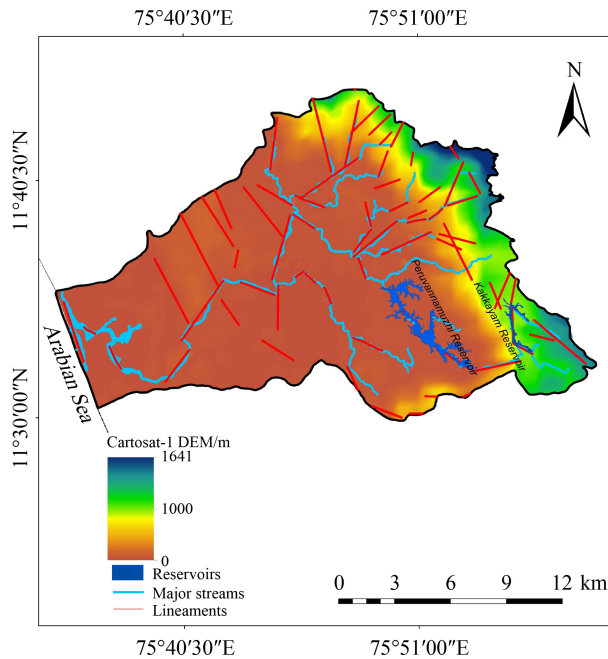


Fig. 1 Kuttiyadi River Basin with major streams, lineaments, elevation details and reservoirs.

3 Materials and methods

In the present investigation, drainage vector data was developed with the aid of image processing software using a resolution of 50 m. KuRB falls in the degree sheet (49M) of sheet Nos. 6, 10, 14, and 15. During preprocessing, the images are georeferenced and mosaiced. Further, the area of interest (AOI) has been extracted through the subset option. The next step is on-screen digitization which was carried out using ArcGIS 10.3 software to demarcate the watershed boundary, sub-watersheds, and stream network. These drainage basins and sub-watersheds which are delineated by tracing the drainage divides on the topographic map. In this river basin, six sub-watersheds are designated, which are SW-I to SW-VI. The order designation technique is the first step for computing the hierarchical anomaly parameters and it is carried out based on the hierarchy ranking of streams proposed by Strahler (1964), whereby fingertip tributaries of streams originate from overland or groundwater flow are designated as a first-order stream. Streams in vector format were ordered according to the Strahler model (Fig. 4). Then the next important step is drainage characteristics analysis; it is a prime factor for hierarchical anomaly analysis to find out the geomorphic process responsible for the evolution of anomalies in the drainage network organization. The drainage pattern of the river basin can be identified from the generated drainage network (Fig. 5). The six sub-watersheds in the basin are delineated by considering drainage divides or ridges and single-stream outlets. The raster DEM was derived from high-resolution Cartosat-1 stereo data which has undergone photogrammetric processing using the LPS (Leica Photogrammetric Suite) tool in ERDAS IMAGINE 2014.

Cartosat-1 DEM data was found to provide more accurate elevation information. The analysis and interpretation of IRS 1D-LISSIII geocoded data products are incorporated in this work for the on-screen digitization and interpretation of the linear and curvilinear features related to tectonic origin (lineaments) and to generate a lineament map (Fig. 1). The methodology for the analysis and interpretation of hierarchical anomaly in the drainage network of KuRB with the aid of the GIS platform is clearly illustrated in the flowchart (Fig. 3).

3.1 Computation of hierarchical anomaly parameters

The hierarchical anomaly in each sub-watershed was evaluated using geospatial technology. When a lower order stream does not merge with its next hierarchical stream order and instead flows to another higher-order stream, an anomaly in the drainage network can result (Anish et al., 2019). After stream ordering, stream junction identification was carried out for the Kuttiyadi river basin and the total number of stream junctions identified for this sixth order basin is 15: 1 → 2, 1 → 3, 1 → 4, 1 → 5, 1 → 6, 2 → 3, 2 → 4, 2 → 5, 2 → 6, 3 → 4, 3 → 5, 3 → 6, 4 → 5, 4 → 6, and 5 → 6 junctions.

To compute the minimum number of streams of various order necessary to make a perfect hierarchical organization of the drainage network, a hierarchical anomaly number in each sub-watershed was calculated (Table 1(a) and Table 1(b)). The hierarchical anomaly in a stream junction can be identified through the ordering of streams; i.e., 1 → 3, 1 → 4, 1 → 5, 1 → 6, 2 → 4, 2 → 5, 2 → 6, 3 → 5, 3 → 6, 4 → 6. The equations (Bahrami, 2013) used to identify hierarchical anomaly parameters in each stream junction is given below.

The equation to calculate hierarchical anomaly number is

$$H_{at\ p-q} = 2(q-2) - 2(p-1), \quad (1)$$

where q is the order of recipient stream segment; p is the order of tributary stream segment.

The equation to calculate hierarchical anomaly number of whole basin/watershed is

$$H_{at} = \sum A_{H_{at\ p-q}} \times B_{NS\ p-q}, \quad (2)$$

where $\sum A_{H_{at\ p-q}}$ is total hierarchical anomaly of each stream junction and $B_{NS\ p-q}$ is the number of streams of each stream junction.

If the hierarchical anomaly number (H_{at}) is higher than the total number of first-order (N_1) streams then the hierarchical anomaly index (Δa) seems to be high. According to Guarnieri and Pirrotta (2008), hierarchical anomaly index is highly sensitive to tectonic effect; it is observed that the Δa parameter is high for tectonically active areas of the Zagros Basin, Iran. The equation to calculate hierarchical anomaly index is

$$\Delta a = H_{at}/N_1, \quad (3)$$

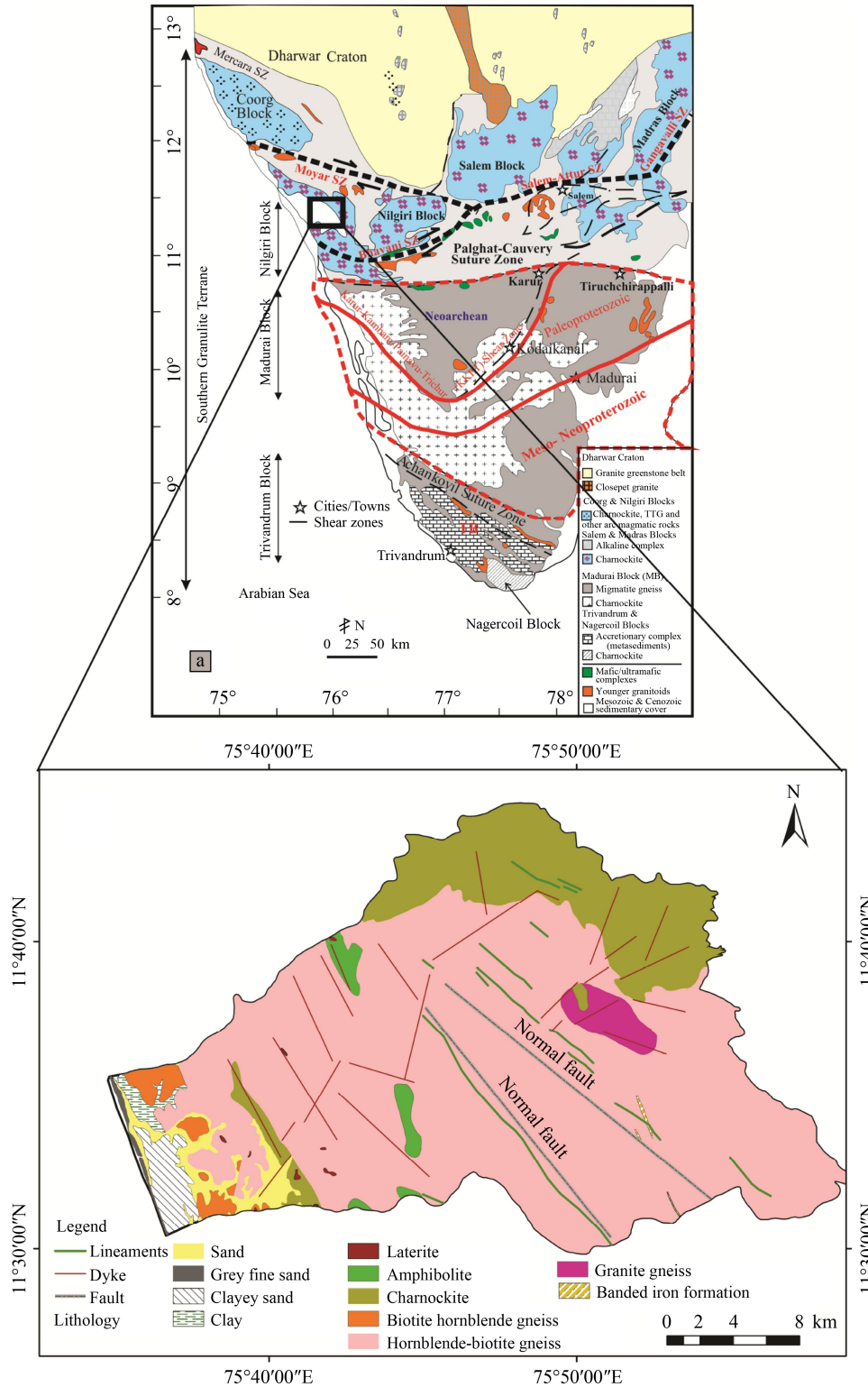


Fig. 2 (a) Major crustal blocks and shear/suture zones in Southern India (modified after Santosh et al. (2015) and Collins et al. (2014)). (b) Lithological map of KuRB.

where N_1 is the total number of first order streams.

3.2 Computation of bifurcation index

Bifurcation index (R) is the difference between the stream

morphometric parameters, bifurcation ratio (R_b), and the direct bifurcation ratio (R_{db}) (Guarnieri and Pirrotta, 2008). Bifurcation ratio (R_b) allows rapid evaluation of the number of streams of a given order (N) to the total number of streams of next higher order in the basin. A

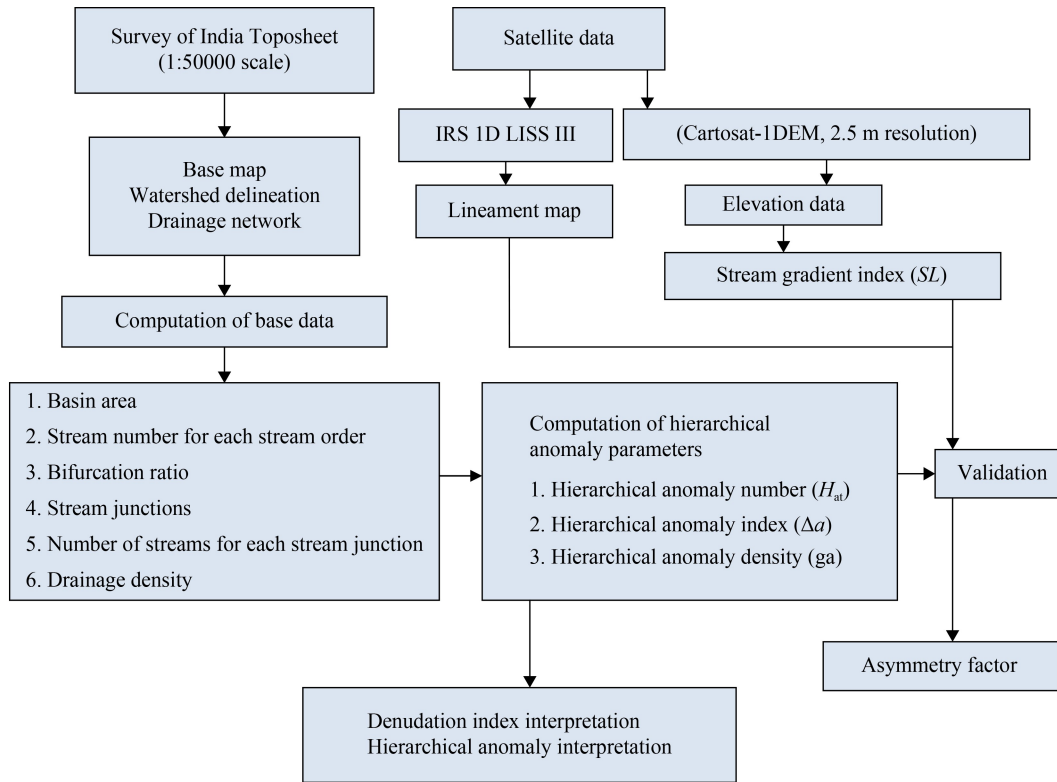


Fig. 3 Workflow diagram of hierarchical anomaly analysis

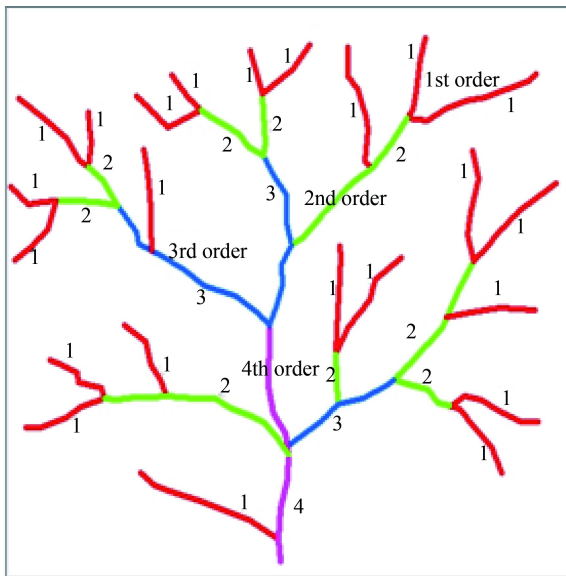


Fig. 4 Stream ordering proposed by Strahler (1964).

high R_b value points to stronger structural control in the drainage network and elongated shape of the basin.

The ratio between the total number of stream segments of a given order which flow to the next higher order ($1 \rightarrow 2$, $2 \rightarrow 3$, $3 \rightarrow 4$, $4 \rightarrow 5$, $5 \rightarrow 6$) stream and the total number of next higher order streams in each sub-watershed are calculated (Table 2(a)) to get direct bifurcation ratio (R_{db}):

$$R_{db} = N_{du}/N_u + 1. \quad (4)$$

Bifurcation index (R) depends on the presence of hierarchical anomalies in the drainage network, the R value of drainage area increases with the increasing number of hierarchical anomalies and hierarchical anomaly indices.

Bifurcation index (Table 2(b)) of the streams is determined by the given equation:

$$R = R_b - R_{bd}. \quad (5)$$

3.3 Computation of stream gradient index and denudation index

The stream gradient index of stream segment ($SL_{segment}$) and for the whole channel (SL_{total}) is determined using elevation details (Fig. 1) from the Cartosat-1 DEM data of the region:

$$SL_{segment} = (\Delta H/\Delta L)L, \quad (6)$$

where $\Delta H = H_1 - H_2$ (elevation difference between higher (H_1) and lower (H_2) elevation points of the major stream channel in a watershed), the horizontal distance between these points is ΔL , and the total length between drainage divide to the midpoint of the major stream segment is L (Prashant and Nirupama, 2016). Then the ratio between ΔH and $\ln L$ (logarithm of the total length of the main stream segment) is used to compute SL_{total} . The ratio between the $SL_{segment}$ to SL_{total} is utilized to predict the anomaly in the drainage network system (Martinez et al., 2011).

To calculate denudation index, the parameters considered are drainage density (D_u) and hierarchical anomaly index (Δa). The drainage density is the measurement of

the ratio of total length of steams of an order to the area of basin expressed in km/km^2 or $\text{miles}/\text{miles}^2$ ($D_d = L_u/A$). A high drainage density indicates closeness of spacing of

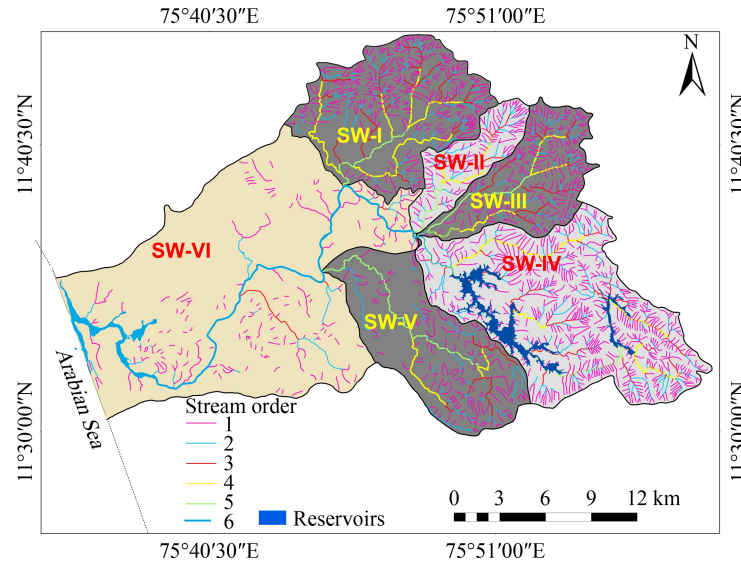


Fig. 5 Sub-watersheds and stream ordering of drainage networks in KuRB.

Table 1(a) Computed stream junctions, number of streams for each stream junction (B) and hierarchical anomaly parameters SW-I to SW-III

Stream junctions	A	SW-I		SW-II		SW-III	
	$H_{at,p \rightarrow q} = 2(q-2) - 2(p-1)$	B	$A \times B$	B	$A \times B$	B	$A \times B$
1-2	0	47	0	27	0	39	0
1-3	1	40	40	6	6	34	34
1-4	3	38	114	11	33	29	87
1-5	7	2	14	5	35	13	91
Total 1st order streams (N_1)		127		49		115	
2-3	0	19	19	8	0	10	0
2-4	2	12	24	3	6	11	22
2-5	6	0	0	4	0	3	18
2-6	14	0	0	0	0	0	0
Total 2nd order streams		31		15		24	
3-4	0	8	0	1	0	4	0
3-5	4	2	8	1	4	2	8
3-6	12	0	0	0	0	0	0
Total 3rd order streams		10		2		6	
4-5	0	3	0	0	0	1	0
4-6	8	0	0	0	0	0	0
Total 4th order streams		3		0		1	
5-6	0	0	0	0	0	0	0
Hierarchical anomaly (H_{at}) = $\sum A \times B$			219		84		260
Hierarchical anomaly index (Δa) $\Delta a = H_{at} / N_1$			1.72		1.71		2.20
Basin area (A)/ km^2		93		29		54	
Hierarchical anomaly density (ga) $ga = H_{at} / A$			2.35		2.89		4.81

Table 1(b) Computed stream junctions, number of streams for each stream junction (*B*) and hierarchical anomaly parameters SW-IV to SW-VI

Stream junctions	<i>A</i>	SW-IV		SW-V		SW-VI		KuRB	
	$H_{a_{p \rightarrow q}} = 2(q-2) - 2(p-1)$	<i>B</i>	<i>A</i> × <i>B</i>	<i>B</i>	<i>A</i> × <i>B</i>	<i>B</i>	<i>A</i> × <i>B</i>	<i>B</i>	<i>A</i> × <i>B</i>
1-2	0	126	0	32	0	13	0	284	0
1-3	1	63	63	9	9	1	1	153	153
1-4	3	75	225	6	18	20	60	179	537
1-5	7	49	343	8	56	0	0	77	539
Total 1st order streams (<i>N</i> ₁)		313		55		33		693	
2-3	0	26	0	5	0	0	0	68	0
2-4	2	13	26	1	2	0	0	40	80
2-5	6	8	48	3	18	0	0	18	108
2-6	14	0	0	0	0	9	26	9	126
Total 2nd order streams		47		9		9		135	
3-4	0	9	0	0	0	0	0	22	0
3-5	4	6	24	0	0	0	0	16	64
3-6	12	0	0	0	0	3	36	3	36
Total 3rd order streams		15		0		3		41	
4-5	0	0	0	0	0	0	0	4	0
4-6	8	3	24	1	8	0	0	4	32
Total 4th order streams		3		1		0	0	8	
5-6	0	0		0		5		5	0
Hierarchical anomaly (H_{at}) = $\sum A \times B$		753		111		122		1675	
Hierarchical anomaly index (Δa)		2.40		2.01		3.69		2.41	
$\Delta a = H_{at}/N_1$									
Basin area (<i>A</i>)/km ²		147		84		268		676	
Hierarchical anomaly density (ga)		5.1		1.32		0.83		2.47	
$ga = H_{at}/A$									

stream segments and it is more likely to occur in regions of structural weak plains or impermeable subsurface material and the area is most prone to high flood peak, surface runoff, and erosion (Chorley, 1969). Denudation is the wearing away of earth surface due to various geomorphic processes; in this study area the high drainage density can augment removal of surface material and to calculate denudation rate the denudation index parameter is utilized. The significant role of weathering and erosion to increase the denudation rate is proven by the past landslide events inventory data and landslide

susceptibility mapping (LSM) of the highlands of this study area (Swetha and Gopinath, 2020).

The formula adopted to calculate denudation index (logTu) is

$$\log Tu = 1.44780 + 0.32619 Du + 0.10247 \Delta a, \quad (7)$$

where Du is drainage density, Δa is hierarchical anomaly index.

Table 2(a) Number of streams in different stream order and joining to next higher order

Sub-watershed	No. of streams in each stream order						No. of streams joining to next higher order					
	1	2	3	4	5	6	1	2	3	4	5	6
SW-I	127	31	10	3	–	–	47	19	8	3	–	–
SW-II	49	15	2	–	–	–	27	8	1	–	–	–
SW-III	115	24	6	1	–	–	39	10	4	1	–	–
SW-IV	313	47	15	3	–	–	126	26	9	–	–	–
SW-V	55	9	–	1	–	–	32	5	–	–	–	–
SW-VI	33	9	3	–	5	1	13	–	–	–	–	–

Table 2(b) Bifurcation index values (R) calculated from bifurcation ratio (R_b) and direct bifurcation ratio (R_{db})

Sub-watershed	Bifurcation ratio (R_b)					Direct Bifurcation ratio (R_{db})						Bifurcation index						
	1/2	2/3	3/4	4/5	5/6	1	2	3	4	5	6	1	2	3	4	5	6	Mean
SW-I	2.7	3.1	3.3	–	–	1.51	1.9	2.66	3	–	–	1.19	1.2	0.67	3	–	–	1.52
SW-II	3.3	7.5	–	–	–	1.8	4	1	–	–	–	1.46	3.5	1	–	–	–	0.99
SW-III	4.8	4	6	–	–	1.62	1.7	4	1	–	–	3.17	2.34	2	1	–	–	2.12
SW-IV	6.7	3.13	5	–	–	2.68	1.7	3	–	–	–	3.97	1.4	2	–	–	–	2.46
SW-V	6.1	9	–	1	–	3.55	5	–	–	–	–	2.56	4	–	1	–	–	2.52
SW-VI	3.7	3	3	5	–	1.4	–	–	–	–	–	2.26	3	3	5	–	–	3.32

4 Result and discussion

To evaluate the hierarchical development of stream networks the KuRB is divided into six sub-watersheds (SW), SW-I (93 km²), SW-II (29 km²), SW-III (54 km²), SW-IV (147 km²), SW-V (84 km²), and SW-VI (268 km²). The hierarchical method of stream ordering proposed by Strahler 1959 is used to determine stream orders and the Kuttiyadi River is identified as a sixth order river which falls in SW-VI. The other five sub-watersheds are characterized with first (SW-I) to fifth (SW-V) order streams.

The lineament map (Fig. 1) and the field evidence (Figs. 6(a)–6(h)) reveals that fracture/joint sets orienting NE–SW through NW–SE seem to play a major role in the behavior of primary streams. These lineaments control the formation of trellis and rectangular patterns (Fig. 5) in the KuRB, which decipher the strong structural influences in the Precambrian basement rocks of the drain area. From the quantitative assessment of the hierarchical organization of each order streams in Kuttiyadi River Basin the parameters such as hierarchical anomaly number (H_{at}), hierarchical anomaly index (Δa), hierarchical anomaly density (ga), and bifurcation index (R) were determined (Tables 1(a), 1(b), and 2). We then evaluated the relevance of these parameters to the tectonic activity which created the anomaly in the drainage network.

4.1 Hierarchical anomaly interpretation

Analysis of hierarchical anomaly parameters throws light on the geomorphic process involved in the evolution of Kuttiyadi Basin, drainage network, and anomalies in the drainage organization. After the hierarchical method of stream ordering, a large difference in the hierarchical organization of streams observed in SW-IV, a total of 631 first-order streams are required to make the drainage network of SW-IV to be in the perfect hierarchical organization. However, the total number of first-order streams observed in the drainage system of SW-IV is only 313. It indicates that destruction of 318 first order stream segments developed a drainage network anomaly in this sub-watershed. Similarly, to make a stream network of the perfect hierarchical organization, 127, 49, 115, 55, and 33 first-order streams are required for SW-I, II, III, V, and VI, respectively.



Fig. 6 (a) Brittle–ductile deformations exposed in the KuRB river bed, SW-I river shows left tilt parallel to the Moyar Shear dextral conjugate movement; (b) conjugate sets of Joints in the SW-II controlled by regional kinematics; (c)–(e) evidence of tectonic signatures and river response to the reactivations of faults/shear Channel migration, unpaired terraces and uplifted river beds; (f)–(h) various joints in the KuRB makes drainage trellis to parallel drainage pattern.

The interpreted value of the hierarchical anomaly index (Δa) is higher for sub-watersheds IV (2.40), III (2.20), and V (2.01) and hierarchical anomaly density (ga) is high for SW-IV (5.1) and SW-III (4.81). From the major

lineament trends and structural weak plains we interpret that the neotectonic activities caused the development of an anomaly in the hierarchical organization of the KuRB drainage network. The values of bifurcation index (R) range between 1 to 3.17 in KuRB sub-watersheds and SW-III, SW-IV, SW-V, and SW-VI show the highest R -value (Table 2(b)). The dominant trellis and rectangular drainage patterns, high values of bifurcation ratio, and bifurcation index values indicate the role of recent tectonic activity for the drainage network organization in the river basin. In this study area high drainage density (3.23, 3.08, and 3.14) and high denudation index values (0.42, 0.40, and 0.43) were determined for SW-II, SW-III, and SW-IV. It suggests that high energy fluvial process induced erosion or diffusion in the stream channel is responsible for destroying the stream segments in these sub-watersheds. Then the construction of Peruvannamuzhi and Kakkayam reservoirs in SW-IV also point toward an anthropogenic reason to alter the drainage network progression here.

The stream gradient index (SL) is used as a proxy to identify the influence of neotectonic activity forming the landscape and landforms. The stream gradient index value of stream segments (SL_{segment}) ranges from 14.67 to 689.90 (Table 3). The peak values of SL_{segment} and SL_{total} in SW-III and SW-IV suggests a sudden change of slope in the upper-midland portion due to imprints of tectonism. It is observed that the ratio of SL_{segment} and SL_{total} ranges from 1.31 to 1.81 in SW-V and SW-VI, and it is due to high energy erosional or diffusion process and its control on stream channel gradient. To validate the tectonic effect in this river basin, asymmetry factor analysis was carried out and a linear regression plot for Δa with A , R_b , R , and SL was used to identify the most influencing parameter

responsible for an increasing Δa index in each sub-watershed.

4.2 Denudation index interpretation

The denudation index of each sub-watershed and for the whole river basin is interpreted from drainage density and hierarchical anomaly index values (Table 4). The high denudation index of 0.40, 0.42, and 0.43 $\text{t}\cdot\text{km}^{-2}\cdot\text{yr}^{-1}$, respectively, was observed in SW-III, SW-II, and SW-IV. The denudation index of KuRB is 0.67 $\text{t}\cdot\text{km}^{-2}\cdot\text{yr}^{-1}$. If the regression plot describing the curve fitness of the hierarchical anomaly index (Δa) and denudation index ($\log Tu$) shows a positive relationship, it indicates that in addition to neo tectonic activity, the role of diffusive process to develop drainage network anomaly (Anish et al., 2019).

5 Validation of findings

The asymmetry factor (AF) analysis is utilized to validate the effect of tectonically induced diffusion in altering drainage network organization in this river basin. If any tectonic deformation occurred it can cause flexure or warping of the topography and the asymmetry factor can be utilized to measure the degree of tilt occurred (Ozkaymak and Sozbilir, 2012). For six sub-watersheds of KuRB the asymmetry factor is measured by dividing the basin area on the right side of the main stream in each sub-watersheds with the total area of that sub-watershed; that is, $AF = (Ar/At)\times 100$, where AF = Asymmetry factor, Ar = basin area on the right bank, and At = total

Table 3 Segments SL index and total length SL index with the ratio in sub-watersheds

SW	ΔH	ΔL	L	SL_{segment}	SL_{total}	$SL_{\text{segment}}/SL_{\text{total}}$
SW-I	25	5.98	14.25	59.57	21.3	2.74
SW-II	5	3.86	11.33	14.67	4.74	3.09
SW-III	360	9.01	13.79	568.96	313.04	1.81
SW-IV	680	16.48	16.72	689.90	556.00	1.73
SW-V	15	12.28	15.88	19.39	12.5	1.55
SW-VI	35	23.87	23.87	35	25.54	1.37

Table 4 Denudation index of sub-watersheds

Sub-watershed	Drainage density	Hierarchical anomaly index (Δa)	Denudation index ($\log Tu$)/($\text{t}\cdot\text{km}^{-2}\cdot\text{yr}^{-1}$)
SW-I	2.79	1.72	0.39
SW-II	3.23	1.71	0.42
SW-III	3.08	2.20	0.40
SW-IV	3.14	2.40	0.43
SW-V	1.65	2.01	0.34
SW-VI	0.66	3.69	2.04
Kuttiyadi basin	2.43	2.41	0.67

area of that basin (Keller and Pinter 1996).

The AF for sub-watersheds I and II is 40% and 47% which shows a left tilt (i.e., NNE). On the other hand, sub-watersheds III, IV, V, and VI show AF values of 72%, 73%, 59%, and 90%, respectively, and tilt toward the right side (i.e., SSE) (Fig. 8). Prasannakumar and McCaig (2016) studies reveal the MoyarBhavani shear having regional tilting of north side up during Paleo-Proterozoic and later south side up during Neo-Proterozoic. These crustal remnant slope factors are still preserved in the form of river tilting and are established through AF. Therefore, the influence of tectonically induced diffusive processes in developing a hierarchical anomaly in the drainage network of this river basin is validated. The morphometric parameters such as drainage density, drainage texture, ruggedness number with high values, and lineaments (Fig. 1) generated for this river basin proved the effect of tectonism in drainage network development and in altering drainage organization.

From the linear relationship of Δa and R , Δa and A , $SL_{segment}/SL_{total}$ ratio, Δa and R_b , Δa and $\log Tu$, and Δa

and AF plotted (Figs. 7(a)–7(f)) and from the R^2 values, a strong relationship exists between Δa to A (0.840), R (0.645), and with AF (0.624). This validates the strong control of these parameters in the increment of the hierarchical anomaly index (Δa). The regression analysis of $\log Tu$ (denudation index) and Δa describe a positive strong relationship with $R^2 = 0.656$ (Fig. 7(e)) and reflects the strong control of the fluvial erosion process in altering the hierarchical organization of streams in sub-watersheds.

6 Conclusions

In this study, quantitative measurement of the hierarchical anomaly parameters, bifurcation index, stream gradient index, and denudation index, with the aid of GIS analysis, throws light upon the anomalies in drainage network development in KuRB and the processes accountable for it. The sub-watersheds of the KuRB show a higher number of anomalies for first and second-order streams.

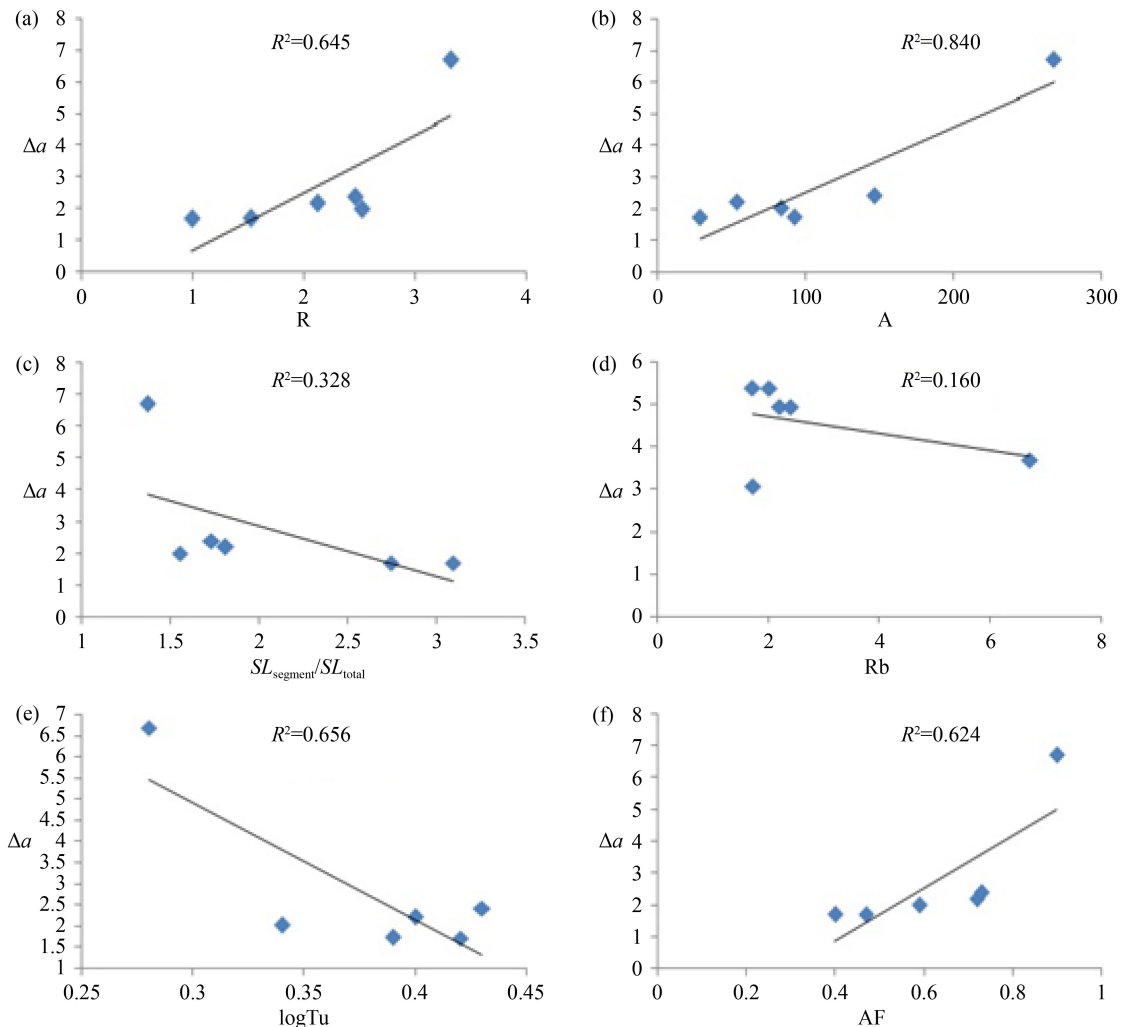


Fig. 7 The interrelationship between (a) Δa and R , (b) Δa and A , (c) Δa and $SL_{segment}/SL_{total}$, (d) Δa and R_b , (e) Δa and $\log Tu$, (f) Δa and AF.

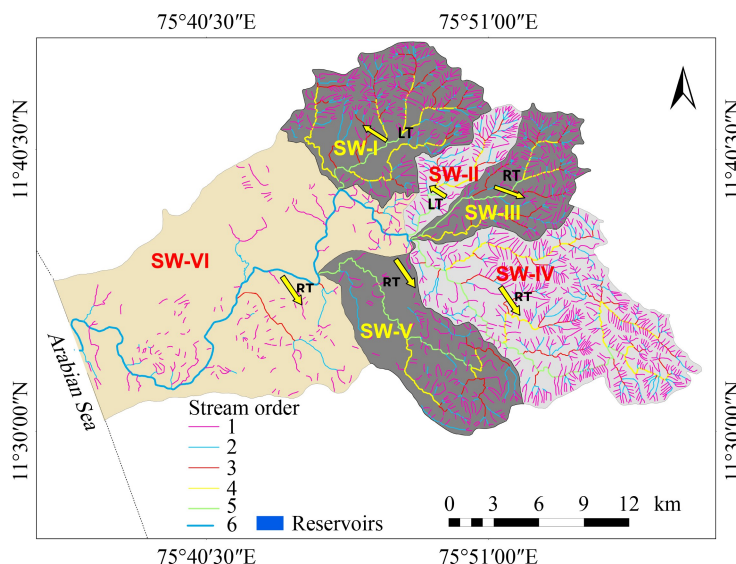


Fig. 8 Kuttiyadi River Basin with drainage networks and tilts direction (yellow arrow toward Right- RT and left- LT side) of sub-watersheds indicate the role of neotectonics.

From the bifurcation index values the higher degree of dissection observed for sub-watersheds III, IV, V, and VI reflects the influence of fluvial erosional processes in these mature (SW-III, SW-IV, and SW-VI) to old stage (SW-V) sub-watersheds in altering the hierarchical organization of the drainage network. Bifurcation index and stream gradient index values provide information about the imprints of tectonism in the drainage network and landscape evolution. The SW-VI encompasses the sixth order stream and has a high R -value of 3.17 and a denudation index of 2.04 result from larger number of lower-order seasonal streams. The sediment yield of the river basin computed is $0.67 \text{ t} \cdot \text{km}^{-2} \cdot \text{yr}^{-1}$. The hierarchical anomaly number (H_{at}) and index (Δa) show high values in SW-III, IV, and VI which indicate deprived hierarchical organization of stream network in these watersheds. It is interpreted that to conquer perfect hierarchical development of a drainage network, 1229 first-order streams, 209 second-order, 80 third-order, and 32 fourth-order streams lack in this river basin. Interpretation of the stream gradient index ($SL_{\text{segment}}/SL_{\text{total}}$) also indicate the stream segment anomalies in all sub-watersheds, steep slope of SW-III and SW-IV, and gentle slope with graded nature of the river in SW-V and SW-VI. Asymmetry factor analysis validated the neo tectonic influence in the drainage network formation especially in upper reach sub-watersheds. Then statistical analysis shows the strong positive relationship of Δa and A , Δa and R , Δa and AF , $\log Tu$, and Δa , which suggest the effect of neo tectonic activity and fluvial erosional processes in creating anomalies in drainage network organization.

Acknowledgment The authors are grateful to the Executive Director, Centre for Water Resources Development and Management (CWRDM), Kozhikode, Kerala, India, for the facilities provided to prepare this manuscript. Thanks also to Mrs. Drishya Girish Bhai, Senior geologist, Geological Survey of India, NER Shillong, for the technical support to prepare this paper.

References

- Ambili V, Narayana A C (2014). Tectonic effects on the longitudinal profiles of the Chaliyar River and its tributaries southwest India. *Geomorphology*, 217: 37–47
- Anish A U, Baiju K R, Midhun E V, Krishnakumar K N (2019). Hierarchical anomaly and denudation index of Karuvannur River Basin, Thrissur District, Kerala, India. *Eco Chronicle*, 14: 60–65
- Bhadran A, Vijesh V K, Gopinath G, Girishbai D, Jesiya N P, Thrikkramji K P (2018). Morpho-hypsometric evolution of the Karuvannur River Basin, a tropical river in central Kerala, southwestern peninsular India. *Arab J Geosci*, 11: 430
- Avena G C, Giuliano G, Palmieri E L (1967). On the quantitative assessment of the hierarchisation and evolution of river networks. *Boll Soc Geol Ital*, 86: 781–796 (in Italian)
- Bahrami S (2013). Analyzing the drainage system anomaly of Zagros basins: implications for active tectonics. *Tectonophysics*, 608: 914–928
- Burbank D, Anderson R (2001). *Tectonic Geomorphology*. Oxford: Blackwell Science
- Bilous L F, Shyshchenko P, Samoilenko V, Havrylenko O (2020). Spatial morphometric analysis of digital elevation model in landscape research. In: *Conference Proceedings, Geoinformatics: Theoretical and Applied Aspects 2020, Vol 2020*
- Chorley R J (1969). *Introduction to Physical Hydrology*, Suffolk Methuen and Co. Ltd.
- Dikpal R L, Renuka Prasad T J, Satish K (2017). Evaluation of morphometric parameters derived from Cartosat-1 DEM using remote sensing and GIS techniques for Budigere Amanikere watershed, Dakshina Pinakini Basin, Karnataka, India. *Appl Water Sci*, 7(8): 4399–4414
- Ghosh S, Sivakumar R (2018). Assessment of morphometric parameters for the development of Relative active tectonic index and its significant for seismic hazard study: an integrated geoinformatic approach. *Environ Earth Sci*, 77: 600
- Gopinath G, Swetha T V, Ashitha M K (2014). Elicitation of erosional

- signature of a tropical river basin with high-resolution stereo data. *App Geoma*, 6(3): 149–157
- Gopinath G, Nair A G, Ambili G K, Swetha T V (2016). Watershed prioritization based on morphometric analysis coupled with multi criteria decision making. *Arab J Geosci*, 9(2): 129
- Guarnieri P, Pirrotta C (2008). The response of drainage basins to the late Quaternary tectonics in the sicilian side of the Messina Strait (NE Sicily). *Geomorphology*, 95(3–4): 260–273
- Hamdouni R E, Irigaray C, Fernández T, Chacón J, Keller E A (2007). Assessment of relative active tectonics, southwest border of Sierra Nevada (Southern Spain). *Geomorphology*, 96(1–2): 150–173
- Horton R E (1941). An approach toward a physical interpretation of infiltration capacity. *Proc Soil Sci Soc Am*, 5(C): 399–417
- Jesiya N, Gopinath G (2018). A fuzzy based MCDM–GIS framework to evaluate groundwater potential index for sustainable groundwater management—a case study in an urban-periurban ensemble, southern India. *Groundw Sustain Dev*, 11: 100466
- Keller E A, Pinter N (2002). *Active Tectonics: Earthquakes, Uplift, and Landscape* (2nd ed). Upper Saddle River: Prentice Hall
- Kumar B A, Gopinath G, Chandran M S S (2014). River sinuosity in a humid tropical river basin, south west coast of India. *Arab J Geosci*, 7(5): 1763–1772
- Kumar D, Duarah B P (2019). Neo-tectonic signatures in the Mishmi Massif, Eastern Himalayas: an interpretation on the basis of the Lohit River Basin geometry. *Arab J Geosci*, 12(21): 665
- Kumar D, Duarah B P (2020). Geomorphic signatures of active tectonics in Subansiri River Basin eastern Himalayas. *J Mt Sci*, 17(6): 1523–1540
- Manu M S, Anirudhan S (2008). Drainage characteristics of Achankovil River Basin, Kerala. *J Geol Soc India*, 71: 841–850
- Marta D S, Maurizio D M, Paola F, Enrico M, Olivia N, Gilberto P, Tommaso P, Francesco T (2008). Morphotectonic evolution of the Adriatic piediment of the Apennines: an advancement in the knowledge of the Marche – Abruzzo border area. *Geomorphology*, 102(1): 119–129
- Martinez M, Hayakawa E H, Stevaux J C, Profeta J D (2011). SI index as indicator of anomalies in the longitudinal profile of Pirapó River. *Geosciences*, 30(1): 63–76
- Nair M M (1990). Structural trendline patterns and lineaments of the Western Ghats, south of 13° Latitude. *J Geol Soc India*, 35: 99–105
- Ozkaymak C, Sozbilir H (2012). Tectonic geomorphology of the Spildagi high ranges western Anatolia. *Geomorphology*, 173–174: 128–140
- Keller E A, Pinter N (1996). *Active Tectonics, Earthquake Uplift and Landscape*. Upper Saddle River: Prentice Hall
- Prasannakumar V, McCaig A M (2016). Reactivation and strain localisation in Bhavani Shear Zone, South India. *J Geol Soc India*, 88(4): 421–432
- Prashant P M, Nirupama P M (2016). Application of Hack's stream gradient index (*SL* index) to longitudinal profiles of the rivers flowing across Satpura-Purna Plain, Western Vidarbha, Maharashtra. *J Indian Geomorph*, 4: 65–72
- Rai P K, Singh P, Mishra V N, Singh A, Sajan B, Shahi A P (2019). Geospatial approach for quantitative drainage morphometric analysis of Varuna river basin, India. *J Landsc Ecol*, 12(2): 1–25
- Rajendran C P, John B, Sreekumari K, Rajendran K (2009). Reassessing the earthquake hazard in Kerala based on the historical and current seismicity. *J Geol Soc India*, 73(6): 785–802
- Ramasamy S M, Kumanan C J, Selvakumar R, Saravanavel J (2011). Remote sensing revealed drainage anomalies and related tectonics of South India. *Tectonophysics*, 501(1–4): 41–51
- Rekha V B, George A V, Rita M (2011). Morphometric analysis and micro-watershed prioritization of Peruvanthanam sub-watershed, the Manimala River Basin, Kerala, South India. *Environ Res Eng Manag*, 57: 6–14
- Santosh M, Yang Q Y, Shaji E, Tsunogae T, Mohan M R, Satyanarayanan M (2015). An exotic mesoarchaeon microcontinent: the Coorg block, southern India. *Gondwana Res*, 27(1): 165–195
- Schumm S A, Dumont J F, Holbrook J M (2000). *Active Tectonics and Alluvial Rivers*. New York: Cambridge University Press
- Soman K (2013). *Geology of Kerala*. Bangalore: Geological Society of India
- Strahler A N (1964). Quantitative geomorphology of drainage basins and channel networks. In: Chow V T, ed. *Handbook of Applied Hydrology*. New York: McGraw-Hill, 439–476
- Swetha T V, Gopinath G, Thrivikramji K P, Jesiya N P (2017). Geospatial and MCDM tool mix for identification of potential groundwater prospects in a tropical river basin, Kerala. *Environ Earth Sci*, 76(12): 428
- Swetha T V, Gopinath G (2020). Landslides susceptibility assessment by analytical network process: a case study for Kuttiyadi River Basin (Western Ghats, southern India). *SN Applied Science*, 2: 1776
- Vijith H, Satheesh R (2006). GIS Based Morphometric analysis of two major upland subwatersheds of Meenachil River in Kerala. *Photonirvachak (Dehra Dun)*, 34(2): 181–185
- Vijith H, Prasannakumar V, Sharath Mohan M A, Ninu Krishnan M V, Pratheesh P (2017). River and basin morphometric indexes to detect tectonic activity: a case study of selected river basins in the South Indian Granulite Terrain (SIGT). *Phys Geogr*, 38(4): 360–378